

ELM energy losses in baseline plasma in JET with the ILW compared to the CFC first-wall

L. Frassinetti¹, D. Dodt², M.N.A. Beurskens³, A. Sirenelli³, T. Eich², J. Flanagan³, C. Giroud³, M. S. Jachmich³, M. Kempenaars³, P. Lomas³, G. Maddison³, R. Neu², I. Nunes⁴, B. Sieglin², and JET-EFDA contributors*

JET-EFDA, Culham Science Centre, Abingdon, OX14 3DB, UK

¹Division of Fusion Plasma Physics, Association EURATOM-VR, KTH, SE-10044 Stockholm, Sweden

²Max-Planck-Institut für Plasma Physik, Boltzmannstr.2, 85748 Garching, Germany

³EURATOM/CCFE Fusion Association, Culham Science Centre, Abingdon, OX14 3DB, UK

⁴Centro de Fusão Nuclear, Associação EURATOM-IST, Lisboa, Portugal

*See appendix of F. Romanelli et al., Fusion Energy, 2012 (24th IAEA Intern. Conference, S. Diego, 2012).

INTRODUCTION

The baseline type I ELM H-mode scenario has been re-established in JET with the new tungsten MKII-HD divertor and beryllium-main wall (hereafter called ITER-like wall, ILW).

In general, the confinement in the ILW plasmas tends to be lower than in the corresponding carbon fibre composite (CFC) wall plasmas [1,2], mainly due to a reduction in the pedestal temperature, as shown in figure 1. A partial recovery to a pedestal pressure comparable to the CFC case has been obtained in high triangularity plasmas with N₂ seeding [3].

The aim of this work is to compare the ELM behaviour in JET with the CFC wall and with the ILW in order to shed light on the confinement differences. The work will focus on the electron temperature (T_e) and density (N_e), on the stored energy and on the ELM time scale.

A set of high ($\delta \sim 0.38-0.42$) and low ($\delta \sim 0.26-0.29$) triangularity discharges characterized by type-I ELMs with $I_p \approx 2.5$ MA and $P_{NBI} \approx 15-18$ MW is considered. For the low δ discharges the D₂ gas fuelling is in the range $\Gamma_{D2} \approx (0.5-1.5) 10^{22}$ e/s in both the CFC and ILW set. For the high δ discharges Γ_{D2} is in the range (1-3) 10^{22} e/s in both the CFC and ILW set. A further group of high δ CFC shots with lower fuelling rate $\Gamma_{D2} < 0.5 10^{22}$ e/s (but with ELM frequency

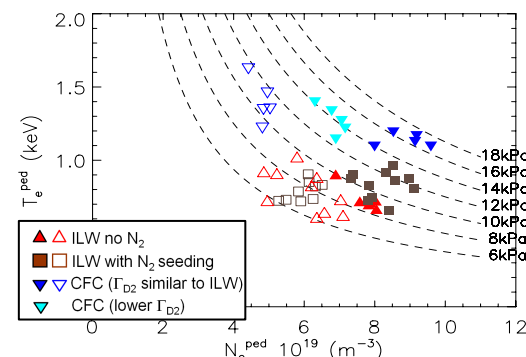


Figure 1. Pedestal electron temperature and density for CFC and ILW shots. Full symbols correspond to the high δ shots and empty symbols to the low δ . Dashed lines highlight the constant pedestal pressure curves.

comparable to the ILW shots) is considered. The electron temperature T_e is measured from the ECE diagnostic and the electron density N_e from reflectometry. When ECE and/or reflectometry were not available, the high resolution Thomson scattering (HRTS) was used. A reasonable agreement between HRTS and ECE/reflectometry is present both in the pre- and post-ELM profiles.

The pedestal T_e and N_e in the pre-ELM phase are shown in figure 1 for all the discharges analysed. High δ ILW shots with N_2 seeding can reach P_e^{ped} up to 13-14kPa, comparable to some CFC shots. Low δ ILW shots with N_2 seeding have P_e^{ped} comparable to the non-seeded low δ ILW shots.

ELM TIME SCALE

The time evolution of T_e^{ped} for three high δ shots is shown in figure 2. The ELM time scale τ_{ELM} is defined as the time interval from the beginning of the ELM collapse to the minimum T_e . The τ_{ELM} calculation is made by considering all the ELMs during a stationary time window.

For the CFC shot, figure 2(a), the T_e collapse is approximately $\tau_{\text{ELM}} \approx 0.8\text{ms}$. For the non-seeded ILW shot, figure 2(b), the T_e behaviour is characterized by an initial collapse with a time scale $\tau_{\text{ELM}} \approx 2.1\text{ms}$. In some cases the T_e collapse is followed by the T_e recovery, while in some cases it is followed by a slower transport event with a $\approx 5\text{-}10\text{ms}$ time scale (note that in the following quantitative analysis this second slow transport

event is not included). For the seeded ILW shot shown in figure 2(c) the time scale is τ_{ELM}

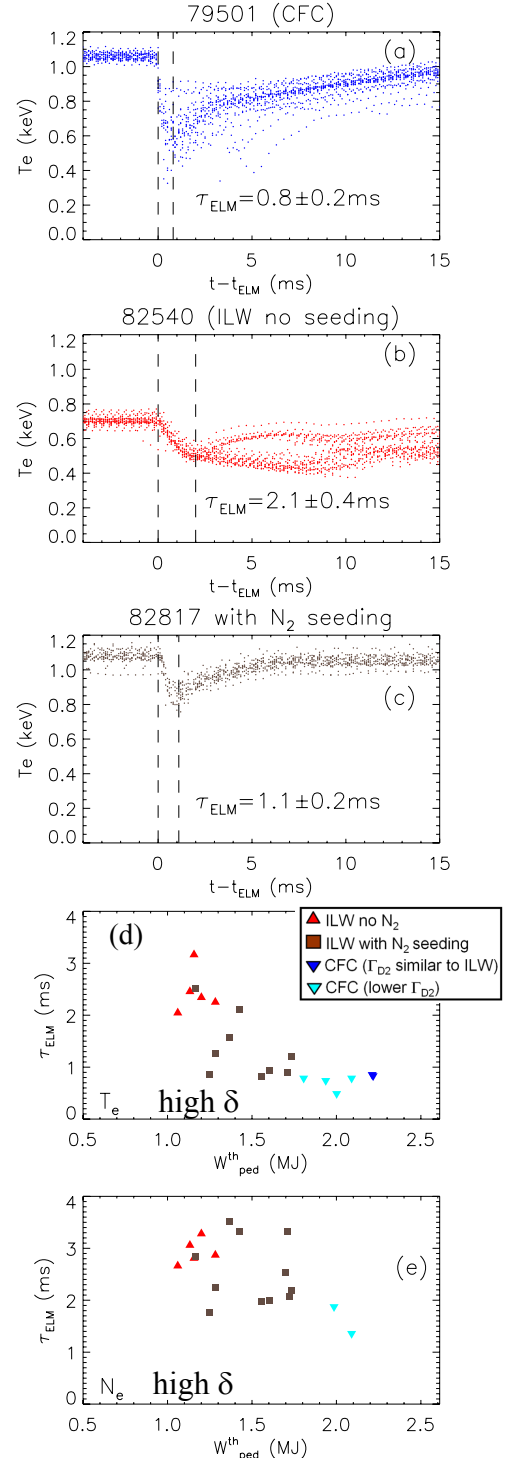


Figure 2. Top frames show the evolution of T_e^{ped} for a CFC (a), a non-seeded ILW (b) and a seeded ILW shot (c). Frames (d) and (e) show the ELM time scale versus the pedestal energy for T_e and N_e (when reflectometry was available) respectively.

≈ 1.1 ms. Note the T_e recovery soon after the ELM and the absence of any further slow transport event as in the unseeded case. Figure 2(d) shows τ_{ELM} versus the pedestal stored energy for the high δ shots. The data suggest that ELMs with fast time scales are characterized by high pedestal energy. In particular, seeded ILW shots can have a time scale for T_e^{ped} comparable to that of the non-seeded ILW shots for $W_{\text{ped}} < 1.5$ MJ and comparable to the CFC shots for $W_{\text{ped}} > 1.5$ MJ. Figure 2(e) shows τ_{ELM} calculated for the electron density for the shots in which reflectometry was available. The τ_{ELM} experimental uncertainty (not shown) is larger than for T_e^{ped} but a relatively similar behaviour can be observed.

For the low δ shots, the ELM time scale is $\tau_{\text{ELM}} \approx 2.0 \pm 0.5$ ms for the non-seeded ILW shots and $\tau_{\text{ELM}} \approx 0.7 \pm 0.4$ ms for the non-seeded CFC shots, i.e. similar to the high δ case. The seeded ILW shots have a time scale comparable to the non-seeded ILW discharges.

ELM ENERGY LOSSES

The pedestal T_e drops, ΔT_e^{ped} , during the ELMs are significantly different between non-seeded ILW and CFC plasmas. As shown in figure 3(a), $\Delta T_e^{\text{ped}} < 0.2$ kev for the ILW discharges while $\Delta T_e^{\text{ped}} > 0.2$ kev for the CFC discharges. Seeded ILW shots can reach ΔT_e^{ped} comparable to the CFC shots. The data suggest a positive trend between ΔT_e^{ped} and T_e^{ped} . The pedestal N_e drops, ΔN_e^{ped} , are also significantly lower for the non-seeded ILW shots (red symbols) than for the CFC shots with similar gas fuelling (dark blue symbols), as shown in figure 3(b). ΔN_e^{ped} for the seeded ILW shots can be instead comparable to the CFC shots, with ΔN_e^{ped} up to $2.2 \cdot 10^{19} \text{ m}^{-3}$.

The ELM energy losses are calculated by volume integrating the T_e and N_e profiles before and after the ELM (in a short time interval near the minimum T_e). Conductive and convective energy losses are calculated as in [4]: $\Delta W_{\text{cond}}^e = \frac{3}{2} \int \Delta T^e n_{\text{pre}}^e dV$, $\Delta W_{\text{conv}}^e = \frac{3}{2} \int \Delta N^e T_{\text{pre}}^e dV$. The results

for high δ plasmas are shown in figure 4(a) and 4(b) respectively. The total ELM energy losses are shown in figure 4(c). For the convective losses, no significant difference is observed between CFC and ILW shots within the experimental uncertainty. Instead, both the

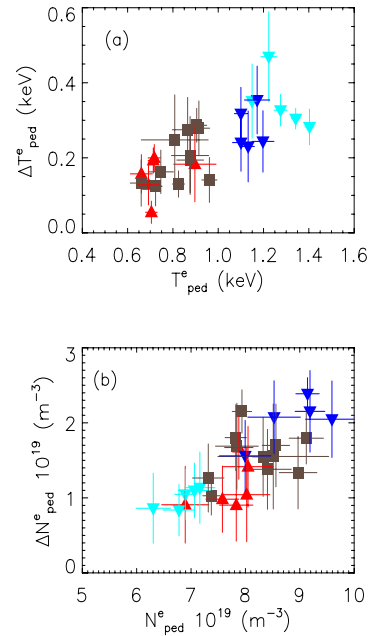


Figure 3. Pedestal drops of electron temperature (a) and electron density (b)

conductive and therefore the total losses are significantly larger for the CFC shots than for the non-seeded ILW shots, while the seeded ILW shots with pedestal energy larger than 1.5MJ can have losses comparable to the CFC shots. The results for low δ plasmas are shown in the bottom row of figure 4. As for the high δ case no significant difference in the convective losses is observed between CFC and ILW shot, frame (e). For the conductive and total losses, the CFC shots are characterized by energy drops larger than the ILW shots. The seeded ILW plasmas have ELM energy comparable to the non-seeded ILW plasmas.

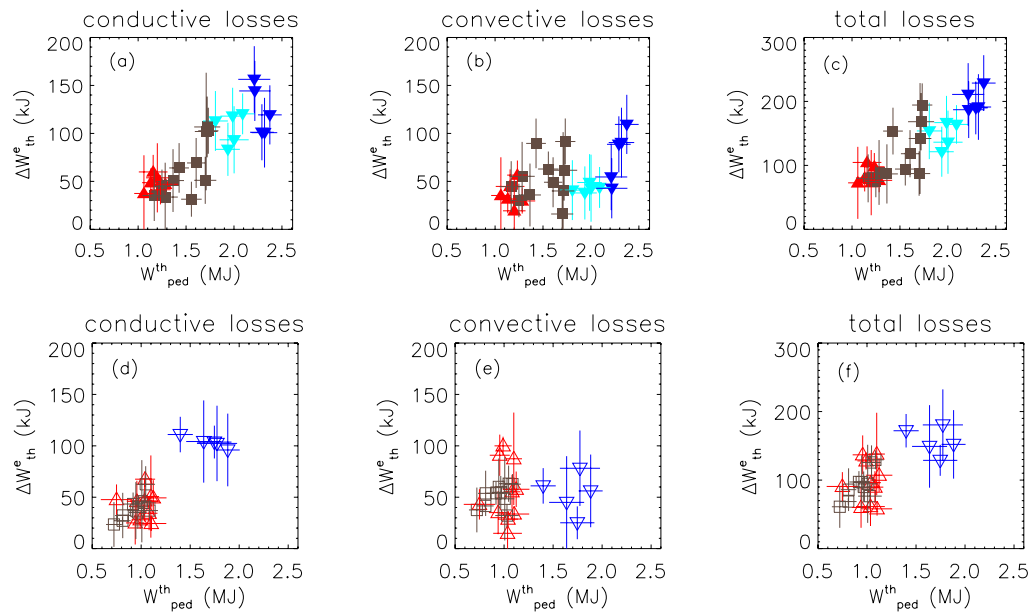


Figure 4. Convective (a,d), conductive (b,e) and total (c,f) ELM energy losses vs pedestal energy for the high triangularity plasmas (top row) and low triangularity plasmas (bottom row).

CONCLUSIONS

The CFC plasmas analyzed in this work are characterized by ELMs with a time scale faster than the non-seeded ILW shots. Moreover, the conductive and therefore the total losses are larger in the CFC shots than in the non-seeded ILW shots. The convective losses are instead similar. However, the seeded ILW shots can reach a confinement comparable to the CFC plasmas. In this case, an ELM behaviour comparable to the CFC discharges (both in terms of time scale and energy losses) is recovered.

ACKNOWLEDGMENTS

This work was supported by EURATOM and carried out within the framework of the European Fusion Development Agreement. The views and opinions expressed herein do not necessarily reflect those of the European Commission.

References

- [1] Frassinetti et al., 39th EPS Conference on Plasma Physics. Stockholm, 2012, P4.072
- [2] Beurskens et al., 24th IAEA Intern. Conference, S. Diego, 2012, EX-P7.20.
- [3] Giroud et al., 24th IAEA Intern. Conference, S. Diego, 2012, EX-P5.30.
- [4] Beurskens et al., Nucl. Fusion **49**, 125006 (2009)